Mech. Engg. Res. Bull.
Vol. 15, (1992), pp. 17-27

EFFECT OF VELOCITY PROFILE ON THE FLOW DEVELOPMENT OF COAXIAL AXISYMMETRIC CONFINED JET.

R. N. Paul *
R. G. M. Hasan *

Abstract

A numerical investigation on the flow development of coaxial axisymmetric confined jet is presented. The boundary layer at the exit from the nozzle (i.e.,inlet condition of the mixing pipe was changed and its effect on the development of flow in the early stages is observed. It was found that for the flow configuration considered, recirculation near the wall is greatly influenced by the exit velocity profile. The effect on turbulence intensity is also significant. It was further observed that as the flow develops downstream, the mean velocity progressively shifts towards a self-preserving profile.

Nomenclature

C_1, C_2, C_μ	:	Empirical constants
G	:	Generation term
k	:	Turbulence intensity, $k = 3/2\ U'^2$
r	:	Radial direction
$r_{1/2}$	:	Half radius : Radius at which mean velocity is half of the centre line velocity.
r_n	:	Radius of primary jet nozzle
r_t	:	Radius of mixing pipe
R_e	:	Reynolds number, $2U_p r_n \rho/\mu$
U_c	:	Centerline velocity
U'	:	Instantaneous turbulence intensity
U_s	:	Average velocity of Secondary stream
U_p	:	Average velocity of Primary stream
U	:	Area mean velocity
u	:	Axial mean velocity
v	:	Radial component of velocity
x	:	Axial direction
X	:	Nondimensional axial distance, x/r_n
μ	:	Absolute viscosity of air
ρ	:	Density of air
δ^*	:	Displacement thickness normalised by r_n
ψ	:	General variable
Γ	:	Diffusivity constant
ε	:	Dissipation rate

Introduction

The flow characteristics in the developing region of coaxial confined jet are dependent on several parameters viz., radius ratio, r_t/r_n (ratio of the radius of the mixing pipe to that of the nozzle; see Fig. 1), velocity ratio, U_s/U_p (ratio of secondary stream velocity to primary jet velocity), swirling pattern of the streams, Reynolds number at the exit from the nozzle etc. Studies reported by Razinsky et al (1), Champagne and Wygnanski (2), Durao and Whitelaw (3), Ko and Lam (4) give an account of the effects of radius ratio, velocity ratio and Reynolds number of coaxial confined jet. Swirling confined jets are also studied by many authors such as Mahmud et al (5).

The confined coaxial jet has some features of free jet and some of the features of entrance flow. It is known from literature that the flow characteristics in the developing region of the free jet (6) as well as entrance flow (7) are significantly dependent on the inlet conditions of the flow(i.e., exit velocity profile of the nozzle). Slight changes in the boundary layer at the exit from the nozzle may affect the flow development. The experimental work of Hasan (8) has reported such a flow configuration where confined coaxial jets were studied by varying the boundary layer at the exit of the nozzle. In the present work, the experiments of Hasan (8) are simulated in an attempt to provide more information on the subtle flow phenomena such as turbulence intensity, flow recirculation near the wall etc. The radius ratio was taken to be 2.5 and the velocity ratio to be 0.023 following Hasan (8). Reynolds number based on the nozzle diameter was taken to be 3.28×10^4. The only variable parameter was the velocity profile (i.e., the thickness of the boundary layer) at the exit from the nozzle.

* Assistant Professor, Mechanical Engineering Deptt. , BUET, Dhaka.

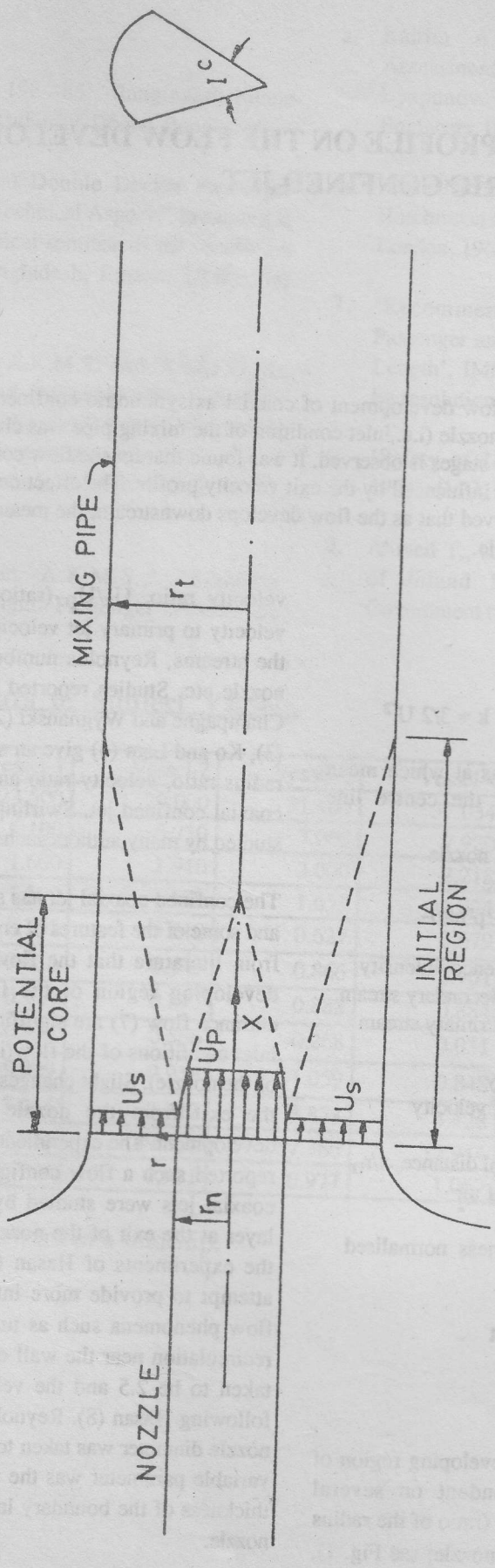

Fig. 1 Schematic diagram of coaxial confined Jet

Mathematical Model

The flow geometry considered in this study (Fig. 1) is axisymmetric and hence a cylindrical-polar mesh is used to cover the flow domain. The governing conservation equations in cylindrical coordinates may be represented by the following single equation:

$$\frac{1}{r}\frac{\partial}{\partial r}(\rho r v \psi) + \frac{\partial}{\partial x}(\rho u \psi) = \frac{1}{r}\frac{\partial}{\partial r}(\Gamma r \frac{\partial \psi}{\partial r}) + \frac{\partial}{\partial x}(\Gamma \frac{\partial \psi}{\partial x}) + S_\psi \qquad (1)$$

where u and v stand for the velocity components in axial (x) and radial (r) directions respectively, ψ is a common variable which has different meaning for different equations. For a particular dependent variable ψ, the appropriate meaning of the diffusion coefficient Γ and the source terms $S\psi$ are summarized in Table 1. To simulate the turbulent flow, a two-equation turbulence model (k-ε) has been employed. The constants appearing in the source terms of k and ε equation (Table 1) are taken to be $C_1 = 1.44$, $C_2 = 1.92$ and $C_\mu = 0.09$ following standard practices.The expression for the generation term, G is given by Eq. 2.

$$G = \Gamma [2\{(\frac{\partial v}{\partial r})^2 + (\frac{\partial u}{\partial x})^2 + (\frac{v}{r})^2\} + \{\frac{\partial u}{\partial r} + \frac{\partial v}{\partial x}\}^2] \qquad (2)$$

In order that a numerical integration can be carried out, the differential equations given by Eq. 1 are to be transformed first into approximate algebraic equations. To do this, the flow domain is divided into small control volumes with a staggered arrangement of velocity components (9). For calculations a non-uniform grid structure of mesh size 70 x 40 (70 in x-direction and 40 in the r-direction) was employed. This particular mesh was selected after several trial runs (10) and this grid was found to yield almost grid independent results.

During the process of discretisation, several assumptions and approximations were made following Patankar (9). In order to extract the pressure field, the SIMPLE (9) algorithm has been adopted. The computer programme used upwind differencing scheme for convection terms. All the computations were done on 80386 computer (ACER, System-15) situated in the Mechanical Engineering Department of Bangladesh University of Engineering and Technology (BUET).

TABLE - 1

Name of equation	Variable ψ	Γ	S_ψ
Continuity	1	0	0
u-momentum	u	μ	$-\frac{\partial p}{\partial x} + \frac{1}{r}\frac{\partial}{\partial r}(\Gamma r \frac{\partial v}{\partial x}) + \frac{\partial}{\partial x}(\Gamma \frac{\partial u}{\partial x})$
v-momentum	v	μ	$-\frac{\partial p}{\partial r} + \frac{1}{r}\frac{\partial}{\partial r}(\Gamma r \frac{\partial v}{\partial r}) + \frac{\partial}{\partial x}(\Gamma \frac{\partial u}{\partial r}) - \frac{2v}{r^2}$
Turbulence Kinetic Energy	k	$\mu + C_\mu \rho k^2/\varepsilon$	$G - \rho\varepsilon$
Dissipation rate	ε	$\mu + C_\mu \rho k^2/\varepsilon$	$C_1 \varepsilon/k\, G - C_2 \rho \varepsilon^2/k$

Results and Discussions

Mean axial velocities at the downstream of the jet for three different exit velocity profiles (Hereafter termed as profile 1, profile 2 and profile 3 as shown in Fig. 2) of the primary jet are shown in Figs. 3a-c for $R_e = 3.28 \times 10^4$ at a velocity ratio of 0.023. For convenience of presentation, the velocity profiles are drawn at axial locations of X = 0, 0.4, 1.4, 3.0, 5.7,7.25 and 9.25. It can be seen that the primary core flow having constant u exists between X = 1.4 and 3.0 for profile 1, whereas it is almost non-existent for profiles 2 and 3. The secondary stream core flow, on the other hand, can be observed only for the first axial location, i.e., X = 0.4. This is due to the fact that Us/Up is very small and hence the secondary flow is very quickly consumed.

The other characteristic feature is the presence of negative velocity near the wall ($r/r_t = 1.0$). For all the three exit profiles of primary jet, there are two negative velocity zones. Stream function plot for profile 1 (Fig. 4) gives a clear picture of the first recirculation on an exaggerated scale. The exact length

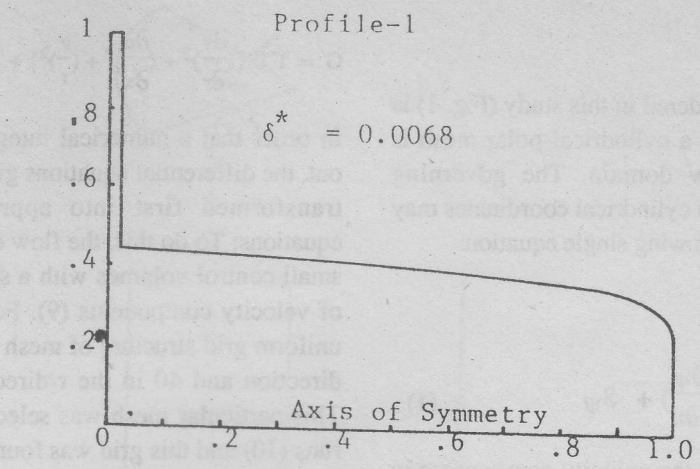

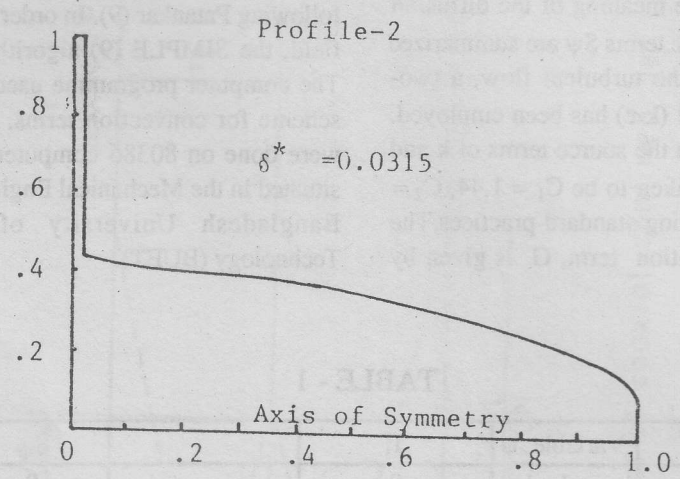

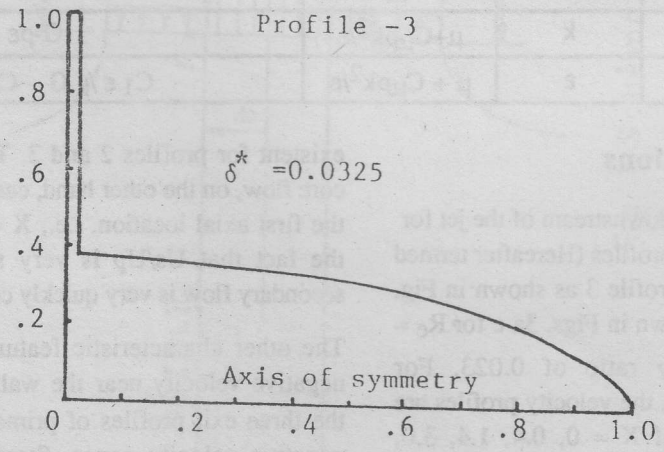

Fig. 2 Inlet velocity profiles of the mixing pipe

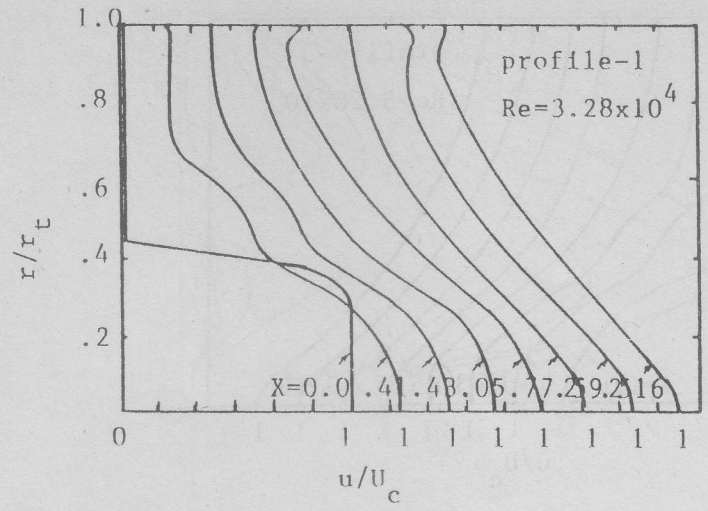

Fig.3.a Mean axial velocity(u/U_c)at different axial locations for profile-1

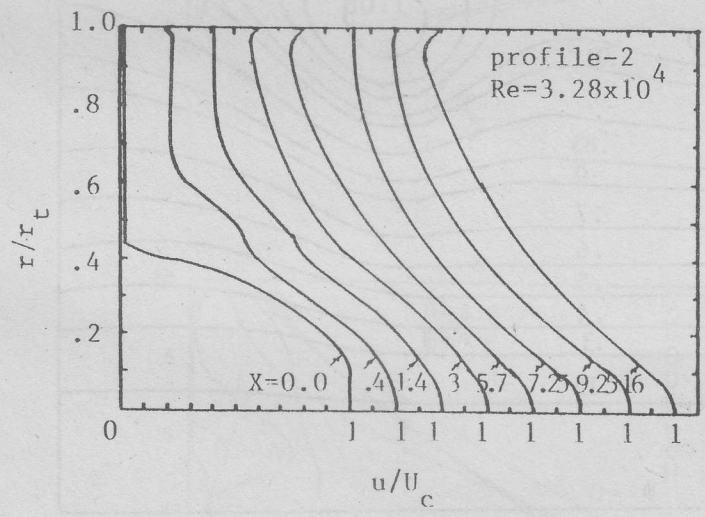

Fig: 3.b Mean axial velocity at different axial locations for profile-2

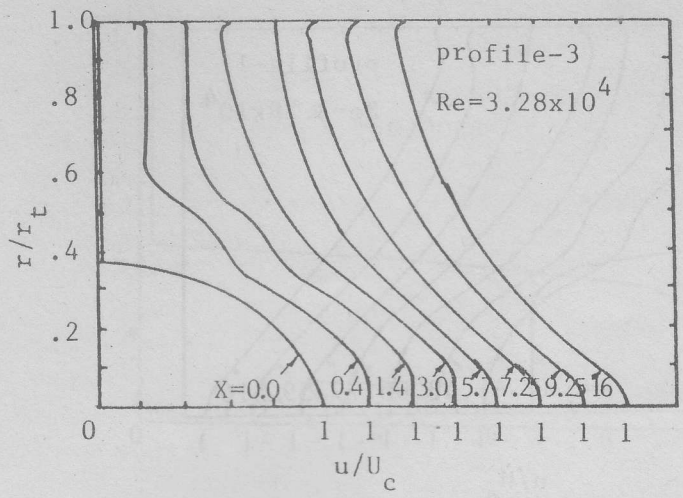

Fig: 3.c Mean axial velocity at different axial locations for profile-3

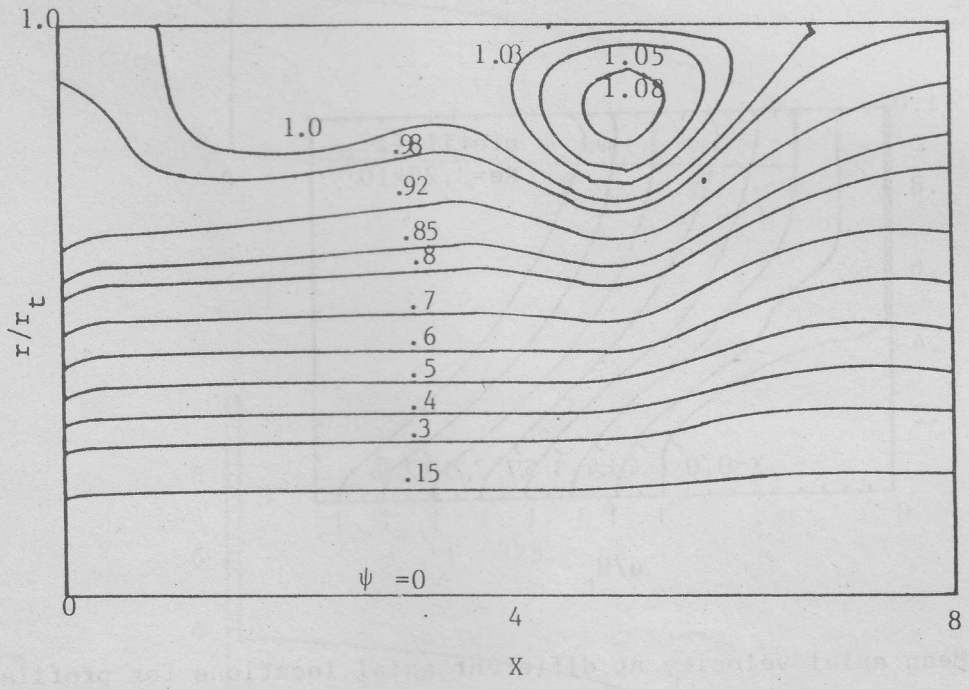

Fig: 4 Contour plot of stream function for profile-1

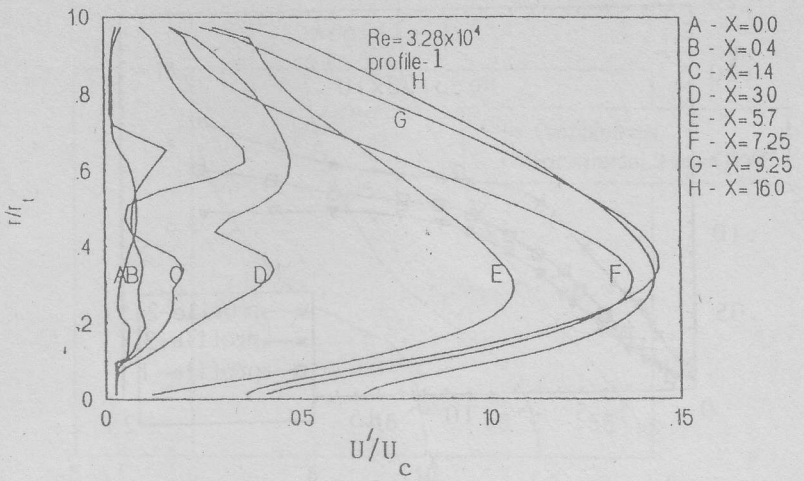

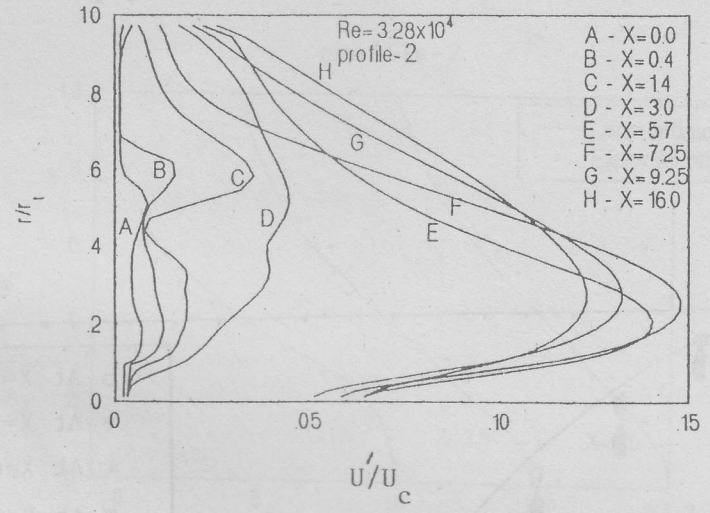

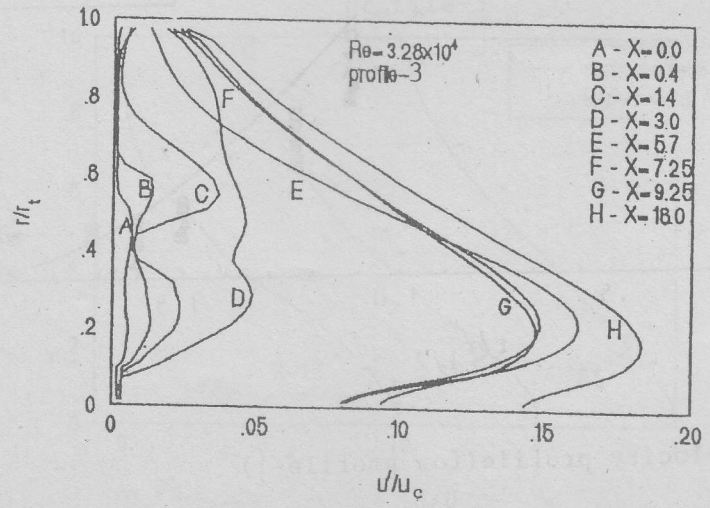

Fig:5 Turbulence intensities at different downstream locations

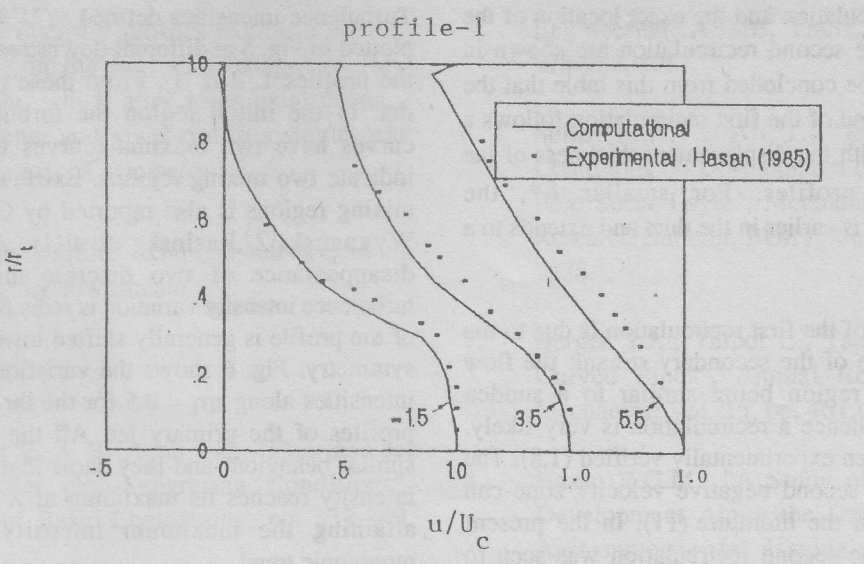

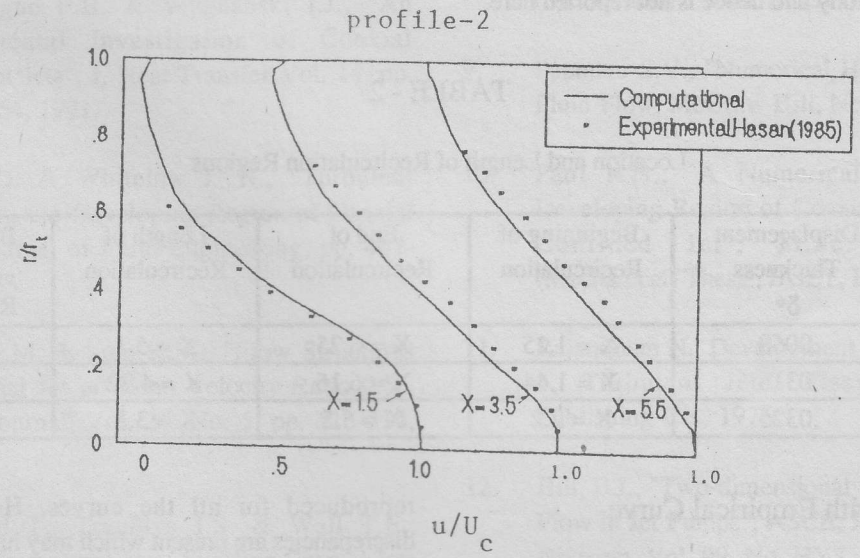

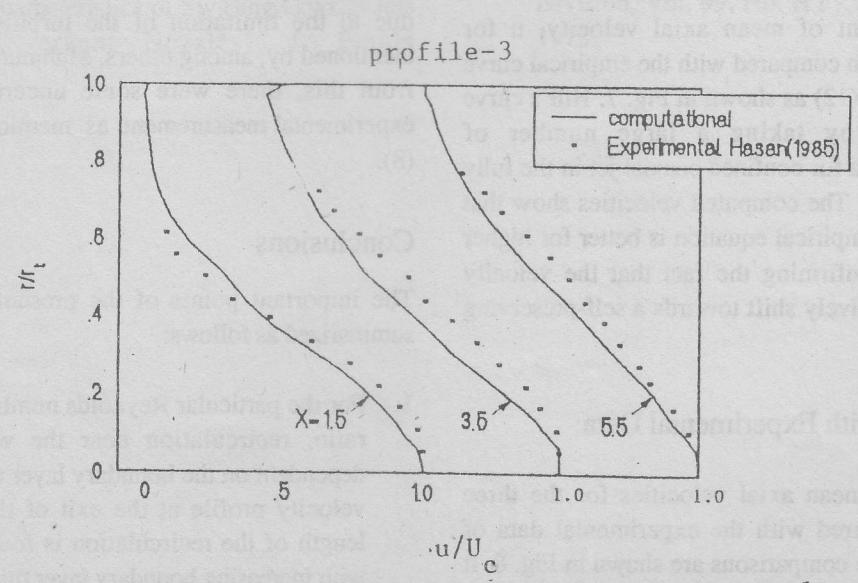

Fig:8 Comparison of u/U_c With Experimental result

of the first recirculation and the exact location of the beginning of the second recirculation are shown in Table 2. It can be concluded from this table that the beginning and end of the first recirculation follows a distinct order with the displacement thickness of the exit velocity profiles. For smaller δ^*, the recirculation starts earlier in the duct and extends to a longer distance.

The occurrence of the first recirculation is due to the small magnitude of the secondary stream: the flow pattern in this region being similar to a sudden expansion, and hence a recirculation is very likely. This has also been experimentally verified (1,8). The possibility of a second negative velocity zone can also be found in the literature (11). In the present investigation, the second recirculation was seen to exist upto X = 30, which is beyond the zone of interest for this study and hence is not reported here.

Turbulence intensities defined as $U' = \sqrt{(2k/3)}$, are plotted in Fig. 5 at different downstream locations for the profiles 1, 2 & 3 . From these plots, it is seen that in the initial region the turbulence intensity curves have two maxima (curves C & D) which indicate two mixing regions. Existence of such two mixing regions is also reported by Champagne and Wygnanski(2),Razinsky et al(1). After complete disappearance of two discrete mixing regions, turbulence intensity variation is reduced and the peak of the profile is generally shifted towards the axis of symmetry. Fig. 6 shows the variation of turbulence intensities along $r/r_t = 0.5$ for the three exit velocity profiles of the primary jet. All the curves exhibit similar behaviour and they show that the turbulence intensity reaches its maximum at X = 7 - 8. After attaining the maximum intensity, it shows a monotonic trend.

TABLE - 2

Location and Length of Recirculation Regions

Exit Profile of Nozzle	Displacement Thickness δ^*	Beginning of Recirculation	End of Recirculation	Length of Recirculation	Beginning of Second Recirculation
1(Fig.2a)	.0068	X = 1.15	X = 6.25	X = 5.1	X = 10.16
2(Fig.2b)	.0315	X = 1.44	X = 6.16	X = 4.72	X = 8.36
3(Fig.2c)	.0325	X = 2.2	X = 5.5	X = 3.3	X = 6.63

Comparison with Empirical Curve

The development of mean axial velocity, u for profile-1 has been compared with the empirical curve proposed by Hill(12) as shown in Fig. 7. Hill's curve was obtained by taking a large number of experimental data for confined coaxial jet in the fully developed stage. The computed velocities show that matching with empirical equation is better for higher values of X, confirming the fact that the velocity profiles progressively shift towards a self-preserving pattern.

Comparison with Experimental Data

The computed mean axial velocities for the three cases are compared with the experimental data of Hasan(8) and the comparisons are shown in Fig. 8. It can be seen that the qualitative nature has been reproduced for all the curves. However, some discrepancies are present which may have been caused due to the limitation of the turbulence model as mentioned by, among others, Mahmud et al(5). Apart from this, there were some uncertainties in the experimental measurement as mentioned by Hasan (8).

Conclusions

The important points of the present study can be summarized as follows:

1. For the particular Reynolds number and velocity ratio, recirculation near the wall is greatly dependent on the boundary layer thickness of the velocity profile at the exit of the nozzle. The length of the recirculation is found to decrease with increasing boundary layer thickness.

2. Turbulence intensity profiles exhibit a double-peak nature in the very early stages of flow development, which after some axial distance merge together and gives rise to a single peak closer to the axis of symmetry.

3. The velocity profiles exhibit a self-preserving nature at further downstream.

References

1. Razinsky E. & Brighton J.A., "Confined Jet Mixing for Non-Separating Conditions", Journal of Basic Engineering, pp. 333-349, 1971.

2. Champagne F.H. & Wygnanski I.J., "An Experimental Investigation of Coaxial Turbulent Jets", J. Heat Transfer Vol. 14, pp. 1445-1464, 1971.

3. Durao D. & Whitelaw J. H., "Turbulent Mixing in the Developing Region of Coaxial Jets", Journal of Fluid Engineering, pp. 467-473, 1973.

4. Ko N.W.M. & Lam K.M., "Flow Structures of Coaxial Jet of Mean Velocity Ratio 0.5", AIAA Journal, Vol. 27, No. 5, pp. 513-514, 1989.

5. Mahmud T., Truelove J.S. & Wall T.F., "Flow Characteristics of Swirling Coaxial Jets from Divergent Nozzles", J. Fluids Engineering, ASME, Trans., Vol. 109, pp. 275-282, 1987.

6. Selim M.A. & Ali T., "Effect of Iintial Conditions on Development of Axisymmetric Free Shear Layer", Mechanical Engineering Research Bulletin, BUET, Vol. 11, pp. 49-59, 1988.

7. Berger S.A., Talbot L., Tao L.S, "Flow in Curved Pipes", Annual Review of Fluid Mechanics, Vol. 15, pp. 461, 1983.

8. Hasan R.G.M., "A Study of Induced Flow Development Along the Downstream of an Axisymmetric Jet Issuing Axially into a Smooth Pipe", M.Sc. Engineering (Mechanical) Thesis, BUET, Dhaka,1985.

9. Patankar S.V., "Numerical Heat Transfer and Fluid Flow, McGraw Hill, New York, 1980.

10. Paul R.N., "A Numerical Study in the Developing Region of Coaxial Axisymmetric Confined Jet", M.Sc. Engineering (Mechanical) Thesis, BUET, Dhaka, 1992.

11. Rajaratnam N., Development in water Science 5, Turbulent Jets, Elsevier Scientific Publishing Co., 1976.

12. Hill, B.J., "Two-dimensional Analysis of Flow in Jet Pumps", ASCE, J. of Hydraulics Division, Vol. 99, No. HY7, pp. 1009-1026, 1973.

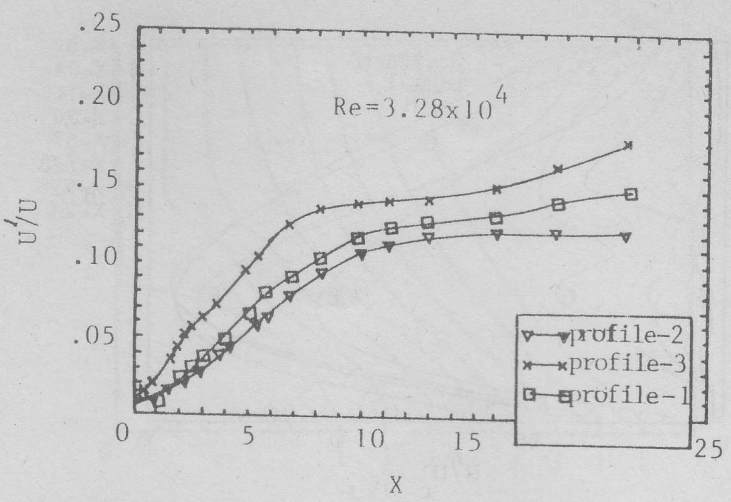

Fig:6 Variation of turbulence intensities along $r_{1/2}$ for profile-1-3

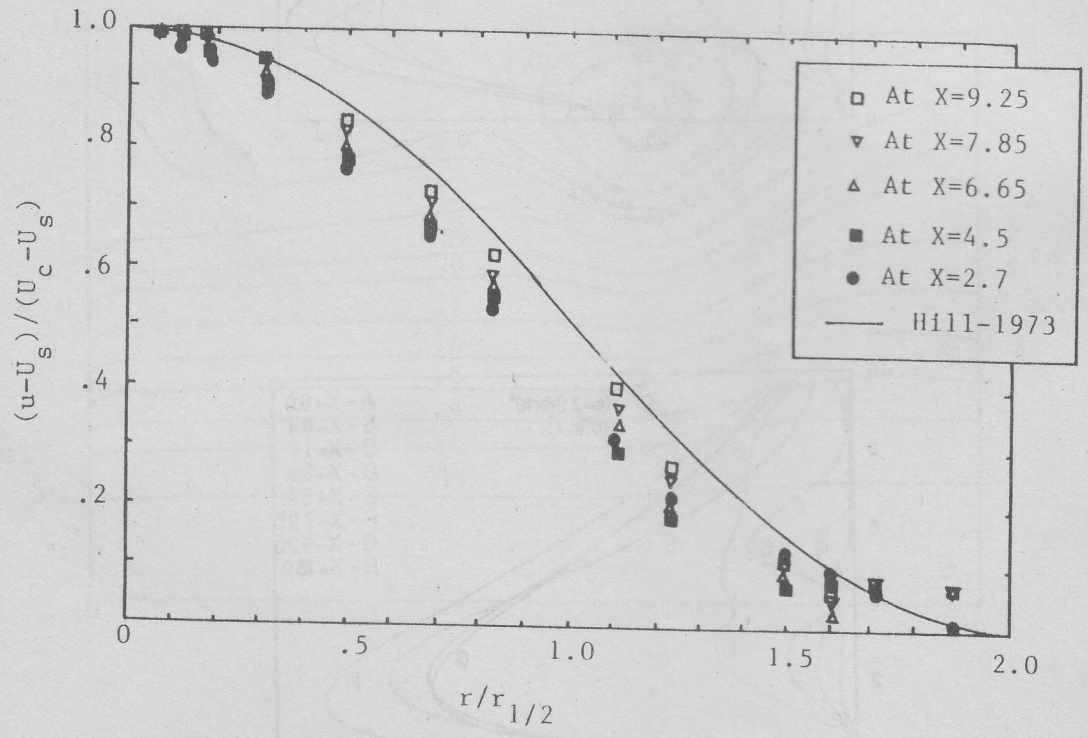

Fig:7 Excess velocity profile(for profile-1)